Varicolored Image De-hazing

Akshay Dudhane, Kuldeep Biradar, Prashant Patil, Praful Hambarde and Subrahmanyam Murala
Computer Vision and Pattern Recognition Lab,
Indian Institute of Technology Ropar, INDIA
2017eez0001@iitrpr.ac.in

Abstract

The quality of images captured in bad weather is often affected by chromatic casts and low visibility due to the presence of atmospheric particles. Restoration of the color balance is often ignored in most of the existing image de-hazing methods. In this paper, we propose a varicolored end-to-end image de-hazing network which restores the color balance in a given varicolored hazy image and recovers the haze-free image. The proposed network comprises of 1) Haze color correction (HCC) module and 2) Visibility improvement (VI) module. The proposed HCC module provides required attention to each color channel and generates color balanced hazy image. While the proposed VI module processes the color balanced hazy image through novel inception attention block to recover the haze-free image. We also propose a novel approach to generate a large-scale varicolored synthetic hazy image database. An ablation study has been carried out to demonstrate the effect of different factors on the performance of the proposed network for image de-hazing. Three benchmark synthetic datasets have been used for quantitative analysis of the proposed network. Visual results on set of real-world hazy images captured in different weather conditions demonstrate the effectiveness of the proposed approach for varicolored image de-hazing.

1. Introduction

Under severe weather conditions, aerosols suspended in the atmosphere greatly absorb and scatter the light rays. Captured images in bad weather appears hazy and are having low visibility. Apparently, color casts of captured images in bad weather often depends upon the size of atmospheric particle and its properties [11]. For example, the mixture of smoke and fog particles causes smoggy weather. Image captured in smog is generally dominated by yellowish and orange color. This varicolored appearance of the haze in captured images may degrade the performance of the high-level computer vision applications. To improve the quality of images captured in inclement weather, image de-hazing is an essential task. The existing image de-hazing approaches [6, 9, 13, 16–19, 21, 28, 30, 31, 36, 37, 39–46] focused mainly on the visibility improvement and ignored the restoration of color balance in de-hazed image. The restoration of color balance is also equally important along with the visibility improvement. Thus, there is a dire need of a versatile image de-hazing approach which is independent of the varicolored haze and is able to restore the color balance along with the visibility improvement in de-hazed image.

Figure 1. Sample real-world varicoloured hazy images and respective haze-free images recovered using the proposed network. (a) and (h) belongs to the grayish dense fog, (b) belongs to the nighttime haze, (c), (f), (g) represents the smog category, (d) is an exceptional case of the sunshine and (e) is a light hazy image.

In this paper, a varicolored end-to-end image de-hazing network is proposed which restores the color balance in given varivolored hazy image and recovers the haze-free image. Sample varicolored hazy images and recovered haze-free images using the proposed network are shown in the Figure 1. Figure 1 witnessed the versatile performance of the proposed network for removal of various (almost all) types of colored haze. In next Section, we have discussed the existing image de-hazing approaches.

2. Literature Survey

Initial approaches in the image de-hazing were directed towards the use of polarized filters [32, 33], multiple images of same scenery [12, 26], handcrafted haze relevant priors [6, 16, 19, 36, 37, 46] etc. Dark channel prior is a baseline haze relevant prior proposed by He *et al.* [19] to get the coarse-level depth information for image de-hazing. However, it fails in sky region and undergoes halo effect near to the complicated edge structures. Since last decade, researchers [9, 13, 28, 30, 31, 39, 40] make use of convolution neural network (CNN) to learn the scene transmission map followed by atmospheric scattering model to recover the haze-free image. Cai *et al.* [9] have proposed deep network to estimate the transmission map followed by atmospheric scattering model to recover the haze-free image. Ren *et al.* [30] proposed holistic transmission map estimation approach for recovery of haze-free scene. Santra *et al.* [31] proposed patch-based comparator for transmission map estimation and recovers the haze-free image when given an information about atmospheric light. These methods optimize only the intermediate feature maps (transmission map and atmospheric light) and do not consider the optimization of the haze-free scene. Thus, errors in each separate estimation step accumulates and magnifes the overall error. In this context, Li *et al.* [21] integrated the transmission map and atmospheric light by reformulating the atmospheric scattering model for image de-hazing. Zhang *et al.* [44] utilized the reformulation proposed in [21] and have proposed the fast multi-scale end-to-end image de-hazing model. Even though these approaches jointly estimate the intermediate feature maps, they still fall under the atmospheric scattering model based approaches and tend to introduce a severe color distortion when tested on varicolored hazy images.

Recently, generative adversarial networks (GANs) shown promising performance in image generation. Yang *et al.* [40] have proposed an end-to-end generative model for image de-hazing. Zhang *et al.* [41] have proposed completely trainable dual generator approach to learn the intermediate feature maps for haze removal. Further, Engin *et al.* [15] utilized robustness of the unpaired conditional GANs to recover the haze-free scene from hazy scene. Since last few years, approaches based on conditional GANs dominating the existing atmospheric scattering model based approaches especially when considering dense haze removal. Dudhane *et al.* [14] proposed an end-to-end trainable residual inception GANs for dense haze removal. Further, Guo *et al.* [18] developed a deep network to jointly estimate the scene transmission map and atmospheric light and further jointly recovered the haze-free image using information from estimated intermediate feature maps.

Research in the single image de-hazing is highly influenced by the use of atmospheric scattering model with an assumption that real-world hazy images posses atmospheric

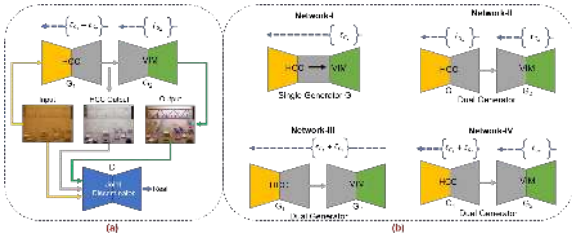

Figure 2. (a) Flow of the proposed varicolored image de-hazing network (b) Different schemes to optimise the Generator 1 and 2.

color constancy *i.e.* they do not have the color imbalance. However, this assumption is not valid for weather conditions like sandstorm, presence of smog etc. Thus, methods which are based on the atmospheric scattering model [19] undergoes the sever color distortion in case of varicolored hazy images. Generative model based approaches [13, 18] show performance improvement at some extent by considering varicolored hazy images in training set. But still they fail to achieve the versatile performance in all types of colored hazy images. Initial work in varicolored image de-hazing is multi-scale fusion approach proposed by Ancuti *et al.* [4, 5]. They derived two inputs by applying white balance and constrast enhancement procedure followed by mutli-scale fusion strategy to recover the haze-free scene. Further, Haung *et al.* [20] have proposed a visibility restoration approach for varicolored haze removal. They utilized the gray world assumption (GWA) [27] to identify whether input hazy image follows color constancy or not. They have reformulated the atmospheric scattering model by incorporating the color difference value with the atmospheric light. Recently, Ren *et al.* [29] have proposed the gated fusion network in which they combinely processed color and contrast corrected maps of the input colored hazy image and followed gating technique to generate the haze-free scene. They make use of GWA algorithm [27] to derive the color correction map of input colored hazy image. It is observed from the existing literature that the approaches designed for varicolored haze removal are highly influenced by white balance algorithms like GWA algorithm. Even though GWA is a simple and effective approach in most of the situations, it is a hand-crafted prior about the color constancy and is not reliable in all cases such as dense haze [4] and brighter part of the image [1]. Thus, effectiveness of the approaches proposed in [20, 29] for image de-hazing is also limited. Thus, there is a dire need of versatile image de-hazing approach which will be applicable to varicolored hazy images.

In this paper, we propose a varicolored image de-hazing approach which restores the color balance and improves the visibility in varicolored hazy images. It is divided into haze color correction (HCC) and visibility improvement (VI) modules. Dual generator and joint discriminator ad-

versarial network is designed to incorporate the HCC and VI modules. Contributions of the proposed work are,

- An end-to-end trainable varicolored image de-hazing network is proposed.
- Haze color correction module is proposed which restores the color balance in varicolored hazy image.
- Visibility improvement module is proposed which process the color balanced hazy image through the novel inception attention block to recover the perceptually pleasant haze-free image.
- A novel approach is proposed to generate a large-scale synthetic varicolored hazy image database.

The proposed network flow is shown in Figure 2 (a). To show the effectiveness of the proposed network for image de-hazing, extensive analysis has been carried out with the help of set of real-world varicolored hazy images and three benchmark synthetic hazy image databases. The proposed approach even works for the night-time image haze-removal without any fine tuning on the night-time hazy images.

3. Proposed Varicolored Image De-hazing

Proposed approach for varicolored image de-hazing is divided into two parts *viz.* 1) Haze color correction module and 2) Visibility improvement module. Figure 3 shows the proposed varicolored image de-hazing network. Details are given in subsequent Sections.

3.1. Haze Color Correction Module

As discussed in Section 1, images captured in the bad weather appears hazy and dominated by the specific color cast. Existing literature [4, 5, 20, 29] employed gray-world assumption (GWA) [27] to restore the color balance in varicolored hazy image. According to the GWA, the average reflectance of the scene (having rich color distribution) is achromatic. One of the simplest method to restore the color balance in an image is to scale the pixel values by a factor $\left(\frac{avg}{avg_c}\right)$ where, avg is a gray value (*global average*) of an image and avg_c represents the illumination color (*i.e. channel-wise average*). Basically, GWA relates the illumination color with the given color distribution only. This might be insufficient when there are brighter regions as well as intense white spots in varicolored hazy image. Figure 4 shows sample varicolored hazy images which are having brighter region as well as intense white spot. Figure 4 witnessed the failure of GWA in marked regions. Thus, extracting robust illumination relevant features may estimate the accurate illumination color and consequently restores the color balance in varicolored hazy image.

We embraced this assumption to propose a novel haze color correction module (HCC). The proposed HCC module restores the color balance in a given varicolored hazy image. Initially, input varicolored hazy image (V) is processed through the channel-wise convolution layer to obtain the pseudo color maps (V_p) as,

$$V_p^i = \{f_i^{3\times3}\left(V^R\right); f_i^{3\times3}\left(V^G\right); f_i^{3\times3}\left(V^B\right)\} \quad (1)$$

where, $\{\cdot\}$ is a concatenation operation along channel axis, R, G, B are the color channels of V, $f^{3\times3}$ represents the convolution operation with filter size of 3×3, i represents number of convolution filters used for each color channel and $i \in \{1:32\}$.

Further, we have imposed the pseudo color correction on each of the pseudo color maps V_p to obtain the refined feature maps (V_r),

$$V_r^c(x) = V_p^c(x) \times \frac{G_p}{I_p(c)}; \quad c \in \{r, g, b\} \quad (2)$$

where, x is an image pixel location, c denotes the color channels of V_p. G_p and $I_p(c)$ represent the gray value and illumination estimate of the V_p respectively and are given as,

$$G_p = \underset{M\times N\times c}{avg} V_p; \qquad I_p(c) = \underset{M\times N}{avg} V_p^c \quad (3)$$

where, $avg_{M\times N\times c}$ is a global average pooling operation, $avg_{M\times N}$ is a spatial pooling operation and is performed on each channel c. M, N represents spatial size and c represents the color channels of V_p.

3.1.1 Restoration of Color Balanced Hazy Image

Unlike GWA, each of the refined feature maps V_r carries information related to the haze color correction. Thus, instead of processing them separately, we thought of blending them to learn the robust features related to the haze color correction. To do so, we concatenate the estimated refined feature maps (V_r) along channel-axis and processed through two encoder blocks to generate the color balanced hazy image. The complete process of the proposed HCC module is shown in Figure 3 (a). Significance of the proposed HCC module is discussed in the ablation study (Section 7). Results of the proposed HCC module and existing GWA approach on sample challenging varicolored hazy images are shown in Figure 4. It is clearly observed that the proposed HCC module restores the color balanced hazy images without affecting the brighter region as well as intense white spot. To the best of our knowledge, this is the first attempt to learn the haze color correction for image de-hazing. This makes proposed approach invariant to the haze color and simplifies the image de-hazing task.

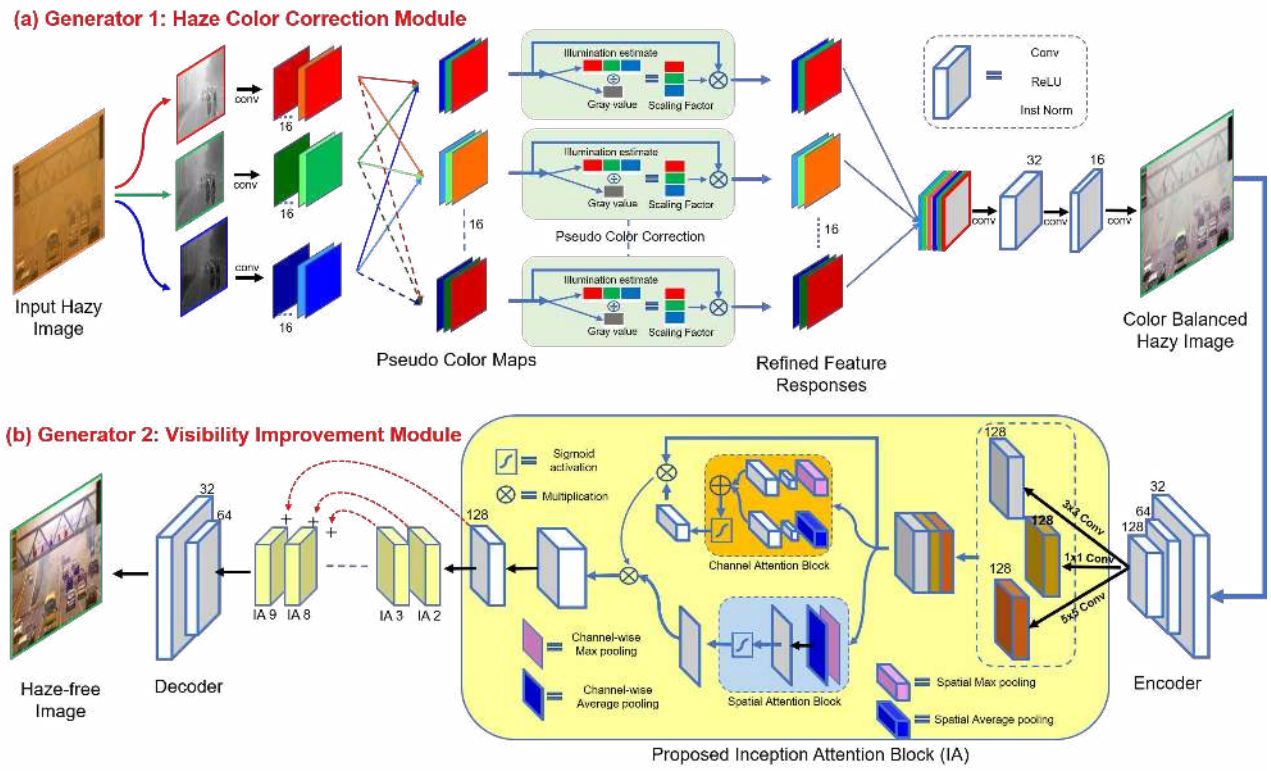

Figure 3. Architecture of the proposed varicolored image de-hazing network. (a) Generator 1 and (b) Generator 2 are aimed to restore the color balanced hazy image and color balanced haze-free image respectively.

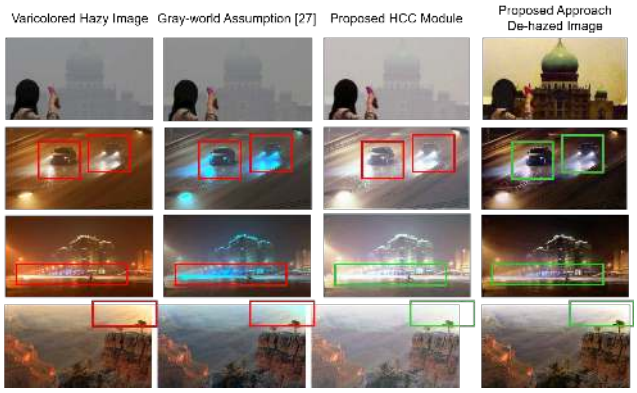

Figure 4. Restoration of the color balance in varicolored hazy image

3.2. Proposed Visibility Improvement Module

Inspired by the success of inception learning [35], we propose an inception attention block to extract the haze relevant features followed by recovery of the haze-free image. Traditional inception block [35] concatenates the feature responce channel-wise and give it to the next stage. Representation power of the inception block can be further improved by giving attention to each feature map along both spatial and channel axes before fetching it to the next stage. Thus, we apply channel and spatial attention modules [38] in parallel paradigm on feature responses of inception convolution filters (shown in Figure 3 (b)). This helps the proposed VI module to flow the haze-relevant features across the network while resist the irrelevant or redundant features. The proposed network comprises of nine inception attention blocks which are connected through the skip connections.

Channel Attention Block: We produce a channel attention map by exploiting the inter-channel relationship of the features. As we know, each channel of a feature map is considered as a feature detector, channel attention focuses more to the robust features while resist the redundant features. To compute the channel-attention coefficient, we squeeze the spatial dimension of the given feature map. To aggregate the spatial information, we make use of both max as well as average pooling. Further, we employed shared network [38] which is composed of multi-layer perceptron to refine the channel-attention coefficient.

Spatial Attention Block: Different from the channel attention, the spatial attention focuses on local informative region. We compute both average and max pooling along channel axes and process through the convolution layer to generate the refined spatial attention map. Whole process of attention mechanism is summarized in Figure 3 (b).

4. Proposed Synthetic Varicolored Hazy Image Database Generation

It is highly impossible to collect a pair of real-world hazy and respective haze-free image. Thus, several synthetic hazy image databases were introduced in the existing literature such as, D-Hazy [2], RESIDE [22], NTIRE [3, 7], HazeRD [45] etc. However, existing datasets lack of varicolored hazy images. NTIRE database has [3, 7] nearly set of 100 varicolored dense foggy image pairs but is limited to slightly bluish and grayish color fog and is not sufficient to train the deep network. Therefore, it is difficult to develop effective deep network for varicolored image de-hazing.

With this motivation, we have constructed a large-scale varicolored hazy image (VHI) database. To train the proposed network, we need varicolored hazy image (Input to Generator 1), color balanced hazy image (Reference image for Generator 1) and haze-free image (Reference image for Generator 2). We follow the benchmark atmospheric scattering model given by Eq. 4 to generate synthetic varicolored and respective color balanced hazy images.

$$V(x) = I(x)\,t(x) + A\,(1 - t(x)) \tag{4}$$

where, x is a pixel location, $I(x)$ is an input haze-free image, $t(x) = exp(-\beta d(x))$ represents scene transmission map, β is an attenuation coefficient, $d(x)$ is a scene depth map, while A represents the atmospheric light.

To generate the synthetic hazy image, information about the scene depth map is essential. With this constraint, we make use of the existing indoor NYU-depth database [34] which has indoor images and respective depth maps.

In Eq. 4, first term denotes the direct attenuation in the visibility, while second term (atmospheric light) denotes the effect of haze and its color cast. Thus, by changing the atmospheric light (A), we can generate the varicolored hazy images. Instead of assuming value of A in Eq. 4, we estimate it from different real-world varicolored hazy images. Channel-wise spatial mean of the real-world varicolored hazy image is considered as an atmospheric light and used in Eq. 4 to generate synthetic hazy images having similar haze color that of respective real-world varicolored hazy image. In this work, we broadly categorized available varicolored hazy images into grayish dense foggy, orange or yellow foggy (smog), bluish foggy and exceptional varicolored hazy images. Turning towards the haze density, here, we use an attenuation coefficient $\beta = \{1, 3, 5\}$ to generate the low, medium and dense synthetic varicolored hazy images respectively. Further, color balanced hazy images for the respective varicolored hazy images are generated by setting $A = (0.8,\ 0.8,\ 0.8)$ and $\beta = \{1, 3, 5\}$.

With the database generation setup discussed above, we have generated 300×8×3 = 7,200 number of synthetic varicolored and color balanced hazy images each where, 300, 8 and 3 represents the number of haze-free indoor images from NYU-Depth database [34], number of real-world varicolored hazy images and level of haze density respectively.

5. Training Details

Synthetically generated VHI database is used to train the proposed network for varicolored image de-hazing. In this work, we have used two generators *viz.* Generator 1 (G_1) and Generator 2 (G_2) for haze color correction and for visibility improvement respectively. Joint discriminator is aimed to discriminate between fake and real responses. As robust performance of the G_2 depends upon the accuracy of the G_1, we allow G_2 loss (ℓ_{G_2}) to jointly update the weight parameters of the G_1 along with G_1 loss (ℓ_{G_1}). Figure 2 (a) and (b) shows the proposed set-up for varicolored image de-hazing and the available options for the weight parameter updation respectively. Details are discussed in ablation study. Weight parameters of the G_1 and G_2 are updated by merging SSIM (l_{SSIM}) [14, 17, 25], and Edge loss (l_{Edge}) [41] along with traditional l_{L_1} loss. We adapt the architecture for discriminator network from [14]. Unlike [14], we assigned discriminator for jointly discriminate between the feature response of HCC and VI modules with their respective reference images as shown in Figure 2 (a).

With this set-up, the proposed network adversarially trained in an end-to-end fashion for varicolored image de-hazing. Hyper-parameters like learning rate = 0.0001, #epochs = 200 are considered. We use NVIDIA DGX station having Intel Xeon E5−2698 and NVIDIA Tesla V100 4×16 GB GPU to train the proposed network.

6. Experimental Analysis

The proposed network is validated for image de-hazing using three benchmark synthetic databases namely 1) Dense-haze [7], 2) D-Hazy [2], 3) Indoor SOTS [22] and set of real-world varicolored hazy images [22]. Average SSIM, PSNR and CIEDE2000 are considered as an evaluation parameters. We compared results of the proposed network with the recently published methods in TPAMI, TIP, CVPR, ICCV, ECCV for image de-hazing.

6.1. Quantitative Evaluation on Synthetic Datasets

Dense haze database [7] images are characterized by bluish illuminaiton and extremly dense haze. The validation set consists of five images of spatial resolution 1200×1600. We follow the NTIRE 2019 de-hazing compitition rules and results of the proposed method are compared quantitatively with the methods those reported their results in the competition [8, 14, 17, 18] along with the recent methods [41,42]. Quantitative evaluation using SSIM and PSNR of the proposed and existing methods is given in Table 1.

	HRDehazer [8] CVPRW-19	DCPDN [41] CVPR-18	PPDNet [42] CVPRW-18	RIGAN [14] CVPRW-19	AtDH+ [18] CVPRW-19	123CEDH+ [17] CVPRW-19	Proposed Method
SSIM	0.5141	0.2593	0.3681	0.5408	0.5395	0.5346	**0.5538**
PSNR	16.47	11.93	13.31	16.47	17.19	17.13	**18.0525**

Table 1. Quantitative Analysis of Image De-hazing on Validation Set of NTIRE2019 [7] Database.

Method	SSIM	PSNR	CIEDE2000
TPAMI-11 [19]	0.7060	12.5876	15.2499
ECCV-16 [28]	0.7231	12.8203	15.8048
ICCV-17 [21]	0.7177	12.4110	16.6565
TIP-18 [31]	0.7300	-	13.0360
TIP-18 [24]	0.7700	-	12.2700
NIPS-18 [40]	0.7726	15.5456	11.8414
CVPRW-18 [15]	0.6490	15.4130	15.0263
CVPRW-19 [14]	0.8179	18.8167	9.0730
Proposed Method	**0.8901**	**23.3142**	**5.9388**

Table 2. Quantitative Analysis of Image De-hazing on D-Hazy [2] Database.

Method	SSIM	PSNR	CIEDE2000
TPAMI-11 [19]	0.8179	16.6215	9.9419
ECCV-16 [28]	0.8102	17.5731	10.7991
ICCV-17 [21]	0.8512	19.0868	8.2716
CVPR-18 [29]	0.8800	22.3113	-
CVPR-18 [41]	0.8378	20.8100	-
TIP-19 [44]	0.9371	27.0100	-
CVPRW-19 [14]	0.8600	21.5600	-
CVPRW-19 [10]	0.9221	24.0200	-
Proposed Method	**0.9511**	**28.2688**	**3.9117**

Table 3. Quantitative Analysis of Image De-hazing on SOTS [22] Database.

Improvement in evaluation parameters show that the proposed method is applicable for the dense haze removal.

D-Hazy database consists of 1,449 synthetic indoor hazy images (generated with fixed attenuation coefficient (β) and atmospheric light A) and respective haze-free indoor images. The proposed network is validated on entire D-Hazy database and results are summerized in Table 2. From Table 2, it is evident that the proposed network outperforms the other existing methods by a large margin for image de-hazing. Unlike D-Hazy database, SOTS database consists of 500 synthetically generated hazy images with different beta (β) factor. All 500 hazy images are considered for the analysis. Table 3 depicts the result of proposed and existing methods on SOTS database. Among all existing methods, FAMED-Net [44] has the second-best average SSIM (0.93) on SOTS database. On the other side proposed network outperforms the FAMED-Net [44] by a margin of 2% in case of SSIM. Also, the proposed network significantly improves the performance in image de-hazing when considering PSNR and CIEDE2000 evaluation parameters.

6.2. Visual Analysis on Real-world Hazy Images

The visual analysis has been carried out on around 3,000 real-world hazy images [22]. Among which set of eight challenging hazy images and recovered haze-free images using the proposed and existing methods are shown in Figure 5. To show the robustness of the proposed network, we considered hazy scenes of various haze color like blue, yellow, gray, white etc. The hazy images characterized by light haze and consisting of large sky region are also considered for the visual evaluation. It can be easily assessed from Figure 5 that existing methods fail on colored haze. The existing methods are able to reduce the effect of haze at some extent. However, they fail to restore the color balance in recovered image. In contrast, the proposed method removes the haze as well as restores the color balance in the recovered haze-free image. We give this credit to the proposed HCC module. The near perfect restoration of the color balance in input varicolored hazy image diluted the level of difficulty in the recovery of haze-free image.

6.3. Night-time Image De-hazing (Cross Domain)

Along with the day-time image de-hazing we validated the proposed network for night-time image haze removal. Fact to notice here is night-time hazy images are not considered in training of the proposed network. Thus, we call this analysis as cross-domain evaluation. Performance of the proposed network is compared with the existing specially designed night-time haze removal approaches [23, 43]. Sample night-time images and respective results are shown in Figure 6. Even in cross domain evaluation, de-hazed results of the proposed network are comparable with the existing [23, 43] approaches.

7. Ablation Study

In this Section, we have demonstrated the effect of different modules on the performance of the proposed network for varicolored image de-hazing.

7.1. HCC Module

To show the significance of the proposed HCC module, we first analyse the results of GWA on set of real-world

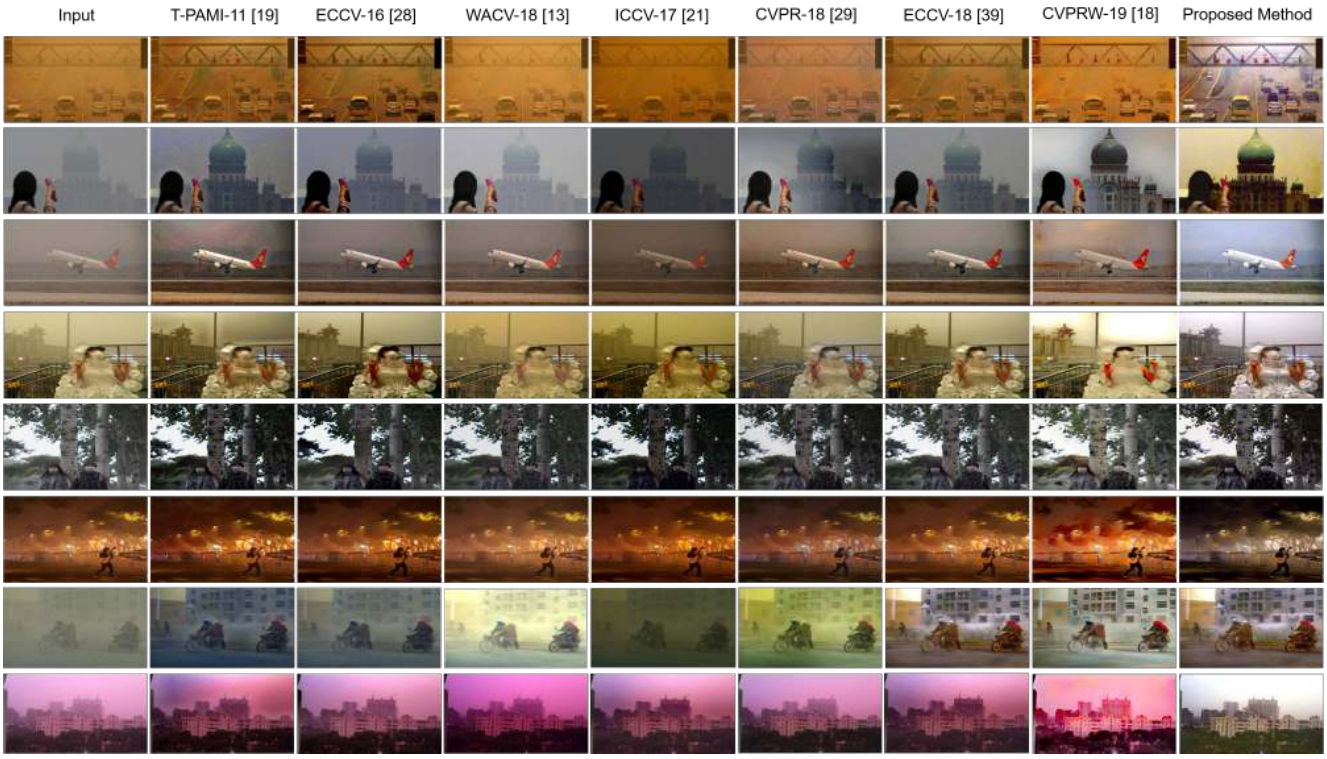

Figure 5. Comparison between the proposed and existing methods for image de-hazing on real-world varicolored hazy images.

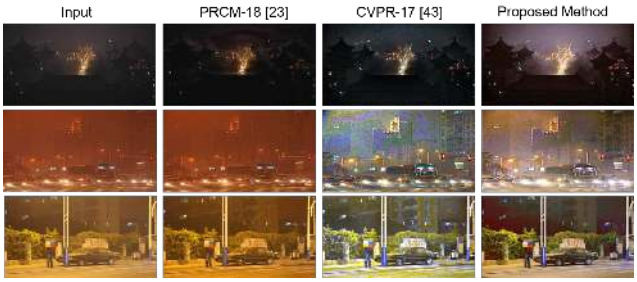

Figure 6. Comparison between the proposed and existing methods for image de-hazing on real-world night-time hazy images.

varicolored hazy images. Sample varicolored hazy images, results of the GWA and results of the proposed HCC module along with the final de-hazed images are shown in Figure 4. It can be observed from the Figure 4 that GWA fails when there are brighter regions as well as intense white spots in varicolored hazy images. The reason behind this could be the insufficient knowledge related to semantic image features, visual attention regions, etc. On the other side, the proposed HCC module robustly learns the illumination correction and restores the near perfect color balance in varicolored hazy image without affecting the brighter and intense white regions. With curiosity about robustness of the proposed HCC module, we analysed its intermediate feature maps *i.e.* the pseudo color maps and their respective refined feature maps obtained from a sample varicolored image (*shown in Figure 7*). It can be observed from Figure 7 that the generated pseudo color maps incorporate both low-level as well as high-level illumination relevant information such as semantic image features, localization of intense white spots, etc. Also, Figure 7 (b) witnessed the refinement in the pseudo color maps *i.e.* separation between the object boundaries, highlighting the brighter and intense white spots etc. We observe that each of these refined feature maps contain complementary and necessary features. Thus, blending of these refined feature responses effectively improved the performance of the proposed HCC module.

We also observed that the restored color balanced hazy images seems slightly hazy but after careful observation, we conclude that it is uniform haze and it may be due to the optimization of the Generator 1 (HCC module) against the color balanced hazy images and not on haze-free images. The proposed visibility improvement module nullifies the effect of this uniform haze. Thus, image de-hazing ability of the proposed network remains unaltered.

7.2. Generator Optimization

In continuation with Section 5, here, we analyse the way of optimization of Generator G_1 and Generator G_2 *viz* i) single generator independent learning (Network-I), ii) two

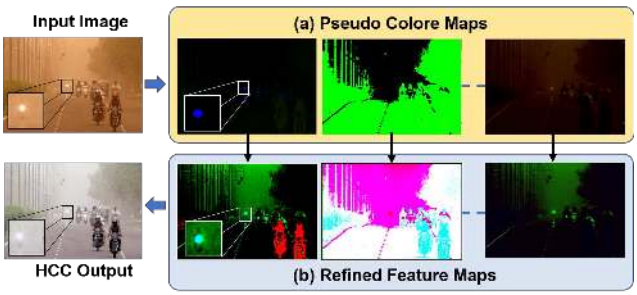

Figure 7. Visualization of intermediate feature maps of the proposed HCC module.

Configuration	SSIM	PSNR
Network-I	0.4572	14.6420
Network-II	0.4834	15.8956
Network-III	0.4902	16.1026
Network-IV	**0.5538**	**18.0225**

Table 4. Quantitative Evaluation of the Different Configurations for Generators Optimization.

Method	SSIM	PSNR
$l_{L_1} + l_{Edge}$	0.4789	14.2580
$l_{L_1} + l_{SSIM}$	0.4879	14.0984
$l_{L_1} + l_{SSIM} + l_{Edge}$	**0.5538**	**18.0225**

Table 5. Quantitative Evaluation of the Proposed Network (Network-IV) with Different Combinations of the Loss Functions

generators and independent learning (Network-II), iii) two generators and combined learning (Network-III), iv) two generators and dependent learning (Network-IV) as shown in Figure 2 (b). An independent learning does optimization of each generator without considering the loss of other generator. While dependant learning optimizes G_1 by considering loss of both $\ell_{G_1} + \ell_{G_2}$. A special case here is, single generator with combined loss. In this, single generator comprises both HCC and VI network architectures in cascaded manner and trained in an end-to-end fashion. Loss of VI module is only considered to optimize both HCC and VI module.

We train these four network configurations on the same training set as discussed in Section 5. Dense haze database [7] is considered for the quantitative evaluation of each configuration and results are summarised in Table 4. It can be observed from Table 4 that the two generators and dependant learning (Network IV) outperforms the other schemes.

7.3. Loss Function

Here, we analyse the effect of loss functions to optimise the proposed network for image de-hazing. We formulate three combinations with SSIM and edge loss by keeping ℓ_{L1} loss common in all combination. Quantitative evaluation of the proposed network when considering these loss combinations while training is given in Table 5. Table 5 witnessed the performance improvement when alone ℓ_{L_1} + SSIM loss is considered than ℓ_{L_1} + edge loss. Whereas the proposed network when optimized by considering all losses outperforms the other combinations.

7.4. Future Scope

Haze correction module is an integral part of the proposed network. It restores the color balance in input varicolored hazy image by learning different illumination relevant features. We observe that the proposed color correction mechanism treats the darkness in the night-time as a color and tries to correct it along with the local illumination sources. This decreases the night-time effect and introduces the pseudo visibility in recovered haze-free image. However, in other sense, at some extent this is an interesting advantage as it may be applicable in night vision applications and further, in future it can be extended for the visibility improvement in dark images.

8. Conclusion

In this work, a varicolored image de-hazing approach is proposed. It consists of haze color correction (HCC) module to restore the color balance in input varicolored hazy image and visibility improvement (VI) module to recover the haze-free image. Proposed HCC module learns the different illumination relevant features and robustly restores the color balance in given varicolored hazy image. Followed by HCC module, the proposed VI module makes use of a novel inception attention block to recover the haze-free image. From analysis on complex scenes, it is observed that the performance of the proposed HCC module remains unaltered in bright regions as well as in intense white objects of the varicolored hazy images. Also, we have constructed a large-scale varicolored hazy image database to train the deep network for varicolored image de-hazing. Quantitative analysis has been carried out on three benchmark synthetic hazy image databases. For visual analysis, real-world hazy images captured in different weather conditions are considered. It is evident from the extensive experimental analysis that the proposed approach is able to restore the color balance as well as is able to recover the haze-free image from all types of varicolored hazy images.

Acknowledgement

Authors would like to thank the anonymous reviewers for their insightful comments and helpful suggestions to improve the quality of this paper. This work was supported by Science and Engineering Research Board (DST-SERB), India, under Grant ECR/2018/001538.

References

[1] Vivek Agarwal, Besma R Abidi, Andreas Koschan, and Mongi A Abidi. An overview of color constancy algorithms. *Journal of Pattern Recognition Research*, 1(1):42–54, 2006.

[2] Cosmin Ancuti, Codruta O Ancuti, and Christophe De Vleeschouwer. D-hazy: A dataset to evaluate quantitatively dehazing algorithms. In *Image Processing (ICIP), 2016 IEEE International Conference on*, pages 2226–2230. IEEE, 2016.

[3] Cosmin Ancuti, Codruta O Ancuti, and Radu Timofte. Ntire 2018 challenge on image dehazing: Methods and results. In *Proceedings of the IEEE Conference on Computer Vision and Pattern Recognition Workshops*, pages 891–901, 2018.

[4] Codruta Orniana Ancuti and Cosmin Ancuti. Single image dehazing by multi-scale fusion. *IEEE Transactions on Image Processing*, 22(8):3271–3282, 2013.

[5] Codruta Orniana Ancuti, Cosmin Ancuti, and Philippe Bekaert. Effective single image dehazing by fusion. In *2010 IEEE International Conference on Image Processing*, pages 3541–3544. IEEE, 2010.

[6] Codruta O Ancuti, Cosmin Ancuti, Chris Hermans, and Philippe Bekaert. A fast semi-inverse approach to detect and remove the haze from a single image. In *Asian Conference on Computer Vision*, pages 501–514. Springer, 2010.

[7] Codruta O Ancuti, Cosmin Ancuti, Mateu Sbert, and Radu Timofte. Dense haze: A benchmark for image dehazing with dense-haze and haze-free images. *arXiv preprint arXiv:1904.02904*, 2019.

[8] Simone Bianco, Luigi Celona, Flavio Piccoli, and Raimondo Schettini. High-resolution single image dehazing using encoder-decoder architecture. In *Proceedings of the IEEE Conference on Computer Vision and Pattern Recognition Workshops*, pages 0–0, 2019.

[9] Bolun Cai, Xiangmin Xu, Kui Jia, Chunmei Qing, and Dacheng Tao. Dehazenet: An end-to-end system for single image haze removal. *IEEE Transactions on Image Processing*, 25(11):5187–5198, 2016.

[10] Shuxin Chen, Yizi Chen, Yanyun Qu, Jingying Huang, and Ming Hong. Multi-scale adaptive dehazing network. In *Proceedings of the IEEE Conference on Computer Vision and Pattern Recognition Workshops*, pages 0–0, 2019.

[11] National Research Council et al. *Protecting visibility in national parks and wilderness areas*. National Academies Press, 1993.

[12] F. Cozman and E. Krotkov. Depth from scattering. In *Proceedings of IEEE Computer Society Conference on Computer Vision and Pattern Recognition*, pages 801–806, Jun 1997.

[13] Akshay Dudhane and Subrahmanyam Murala. C^2msnet: A novel approach for single image haze removal. In *Applications of Computer Vision (WACV), 2018 IEEE Winter Conference on*, pages 1397–1404. IEEE, 2018.

[14] Akshay Dudhane, Harshjeet Singh Aulakh, and Subrahmanyam Murala. Ri-gan: An end-to-end network for single image haze removal. In *Proceedings of the IEEE Conference on Computer Vision and Pattern Recognition Workshops*, pages 0–0, 2019.

[15] Deniz Engin, Anil Genc, and Hazim Kemal Ekenel. Cycle-dehaze: Enhanced cyclegan for single image dehazing. In *Proceedings of the IEEE Conference on Computer Vision and Pattern Recognition Workshops*, pages 825–833, 2018.

[16] Raanan Fattal. Single image dehazing. *ACM Transactions on Graphics (TOG)*, 27(3):72, 2008.

[17] Tiantong Guo, Venkateswararao Cherukuri, and Vishal Monga. Dense123'color enhancement dehazing network. In *Proceedings of the IEEE Conference on Computer Vision and Pattern Recognition Workshops*, pages 0–0, 2019.

[18] Tiantong Guo, Xuelu Li, Venkateswararao Cherukuri, and Vishal Monga. Dense scene information estimation network for dehazing. In *Proceedings of the IEEE Conference on Computer Vision and Pattern Recognition Workshops*, pages 0–0, 2019.

[19] Kaiming He, Jian Sun, and Xiaoou Tang. Single image haze removal using dark channel prior. *IEEE Transactions on Pattern Analysis and Machine Intelligence*, 33(12):2341–2353, 2011.

[20] Shih-Chia Huang, Bo-Hao Chen, and Wei-Jheng Wang. Visibility restoration of single hazy images captured in real-world weather conditions. *IEEE Transactions on Circuits and Systems for Video Technology*, 24(10):1814–1824, 2014.

[21] Boyi Li, Xiulian Peng, Zhangyang Wang, Jizheng Xu, and Dan Feng. Aod-net: All-in-one dehazing network. In *Proceedings of the IEEE International Conference on Computer Vision*, pages 4770–4778, 2017.

[22] Boyi Li, Wenqi Ren, Dengpan Fu, Dacheng Tao, Dan Feng, Wenjun Zeng, and Zhangyang Wang. Benchmarking single-image dehazing and beyond. *IEEE Transactions on Image Processing*, 28(1):492–505, 2019.

[23] Yinghong Liao, Zhuo Su, Xiangguo Liang, and Bin Qiu. Hdp-net: Haze density prediction network for nighttime dehazing. In *Pacific Rim Conference on Multimedia*, pages 469–480. Springer, 2018.

[24] Qi Liu, Xinbo Gao, Lihuo He, and Wen Lu. Single image dehazing with depth-aware non-local total variation regularization. *IEEE Transactions on Image Processing*, 27(10):5178–5191, 2018.

[25] Peter Morales, Tzofi Klinghoffer, and Seung Jae Lee. Feature forwarding for efficient single image dehazing. In *Proceedings of the IEEE Conference on Computer Vision and Pattern Recognition Workshops*, pages 0–0, 2019.

[26] Shree K Nayar and Srinivasa G Narasimhan. Vision in bad weather. In *Computer Vision, 1999. The Proceedings of the Seventh IEEE International Conference on*, volume 2, pages 820–827. IEEE, 1999.

[27] Erik Reinhard, Michael Adhikhmin, Bruce Gooch, and Peter Shirley. Color transfer between images. *IEEE Computer graphics and applications*, 21(5):34–41, 2001.

[28] Wenqi Ren, Si Liu, Hua Zhang, Jinshan Pan, Xiaochun Cao, and Ming-Hsuan Yang. Single image dehazing via multi-scale convolutional neural networks. In *European Conference on Computer Vision*, pages 154–169. Springer, 2016.

[29] Wenqi Ren, Lin Ma, Jiawei Zhang, Jinshan Pan, Xiaochun Cao, Wei Liu, and Ming-Hsuan Yang. Gated fusion network for single image dehazing. In *The IEEE Conference on Computer Vision and Pattern Recognition (CVPR)*, June 2018.

[30] Wenqi Ren, Jinshan Pan, Hua Zhang, Xiaochun Cao, and Ming-Hsuan Yang. Single image dehazing via multi-scale convolutional neural networks with holistic edges. *International Journal of Computer Vision*, pages 1–20, 2019.

[31] Sanchayan Santra, Ranjan Mondal, and Bhabatosh Chanda. Learning a patch quality comparator for single image dehazing. *IEEE Transactions on Image Processing*, 27(9):4598–4607, 2018.

[32] Yoav Y Schechner, Srinivasa G Narasimhan, and Shree K Nayar. Instant dehazing of images using polarization. In *Computer Vision and Pattern Recognition, 2001. CVPR 2001. Proceedings of the 2001 IEEE Computer Society Conference on*, volume 1, pages I–I. IEEE, 2001.

[33] S. Shwartz, E. Namer, and Y. Y. Schechner. Blind haze separation. In *2006 IEEE Computer Society Conference on Computer Vision and Pattern Recognition (CVPR'06)*, volume 2, pages 1984–1991, 2006.

[34] Nathan Silberman, Derek Hoiem, Pushmeet Kohli, and Rob Fergus. Indoor segmentation and support inference from rgbd images. In *European Conference on Computer Vision*, pages 746–760. Springer, 2012.

[35] Christian Szegedy, Wei Liu, Yangqing Jia, Pierre Sermanet, Scott Reed, Dragomir Anguelov, Dumitru Erhan, Vincent Vanhoucke, and Andrew Rabinovich. Going deeper with convolutions. In *Proceedings of the IEEE conference on computer vision and pattern recognition*, pages 1–9, 2015.

[36] Robby T Tan. Visibility in bad weather from a single image. In *Computer Vision and Pattern Recognition, 2008. CVPR 2008. IEEE Conference on*, pages 1–8. IEEE, 2008.

[37] Ketan Tang, Jianchao Yang, and Jue Wang. Investigating haze-relevant features in a learning framework for image dehazing. In *Proceedings of the IEEE Conference on Computer Vision and Pattern Recognition*, pages 2995–3000, 2014.

[38] Sanghyun Woo, Jongchan Park, Joon-Young Lee, and In So Kweon. Cbam: Convolutional block attention module. In *The European Conference on Computer Vision (ECCV)*, September 2018.

[39] Dong Yang and Jian Sun. Proximal dehaze-net: a prior learning-based deep network for single image dehazing. In *Proceedings of the European Conference on Computer Vision (ECCV)*, pages 702–717, 2018.

[40] Xitong Yang, Zheng Xu, and Jiebo Luo. Towards perceptual image dehazing by physics-based disentanglement and adversarial training. In *In Thirty third-second AAAI conference on Artificial Intelligence (AAAI-18)*, 2018.

[41] He Zhang and Vishal M Patel. Densely connected pyramid dehazing network. In *Proceedings of the IEEE conference on computer vision and pattern recognition*, pages 3194–3203, 2018.

[42] He Zhang, Vishwanath Sindagi, and Vishal M Patel. Multi-scale single image dehazing using perceptual pyramid deep network. In *Proceedings of the IEEE Conference on Computer Vision and Pattern Recognition Workshops*, pages 902–911, 2018.

[43] Jing Zhang, Yang Cao, Shuai Fang, Yu Kang, and Chang Wen Chen. Fast haze removal for nighttime image using maximum reflectance prior. In *Proceedings of the IEEE Conference on Computer Vision and Pattern Recognition*, pages 7418–7426, 2017.

[44] J. Zhang and D. Tao. Famed-net: A fast and accurate multi-scale end-to-end dehazing network. *IEEE Transactions on Image Processing*, 29:72–84, 2020.

[45] Yanfu Zhang, Li Ding, and Gaurav Sharma. Hazerd: an outdoor scene dataset and benchmark for single image dehazing. In *2017 IEEE International Conference on Image Processing (ICIP)*, pages 3205–3209. IEEE, 2017.

[46] Qingsong Zhu, Jiaming Mai, and Ling Shao. Single image dehazing using color attenuation prior. In *25th British Machine Vision Conference, BMVC 2014*, 2014.